

Subgraph-based filterbanks for graph signals

Nicolas Tremblay, Pierre Borgnat, *Member, IEEE*

Abstract—We design a critically-sampled orthogonal transform for graph signals, via graph filterbanks. Instead of partitioning the nodes in two sets so as to remove one every two nodes in the filterbank downsampling operations, the design is based on a partition of the graph in connected subgraphs. Coarsening is then achieved by defining one “supernode” for each subgraph: the edges for this coarsened graph derives hence from connectivity between the subgraphs. Unlike the one every two nodes downsampling operation on bipartite graphs, this coarsening operation does not have an exact formulation in the Fourier space of the graph. Instead, we rely on the local Fourier bases of each subgraph to define filtering operations. We apply successfully this method to decompose graph signals, and show promising performance on compression and denoising experiments.

Index Terms—Graph signal processing, Laplacian pyramid, filterbanks, community detection, wavelet.

I. INTRODUCTION

Graphs are a modeling tool suited to many applications involving networks, may they be social, neuronal, or driven from computer science, molecular biology [1]... Data on these graphs may be defined as a scalar (or vector) on each of its node, forming a so-called *graph signal* [2]. In a sense, a graph signal is the extension of the 1-D discrete classical signal (where the signal is defined on the circular graph, each node having exactly two neighbors) to any arbitrary discrete topology where each node may have an arbitrary number of neighbors. Temperature measured by a sensor network, age of the individuals in a social network, Internet traffic in a router network, etc. are all examples of such graph signals.

Adapting classical signal processing tools to signals defined on graphs have raised significant interests in the last few years [2], [3]. For instance, the graph Fourier transform, the usual building block of signal processing methods, has several possible definitions, either based on the diagonalisation of one of the graph’s Laplacian matrix [4], or based on Jordan’s decomposition of the adjacency matrix [5], [6]. Building upon this graph Fourier transform, authors have defined different interpolation procedures [7]–[9], windowed Fourier transform [10], graph empirical mode decomposition [11], different wavelet transforms, including spectral graph wavelets [4], [12], [13], diffusion wavelets [14], and wavelets defined via filterbanks [15]–[18]. Among the applications of graph signal processing, one may cite works on fMRI data [19], on multi-scale community detection [20], image compression [21] etc... In fact, such graph signal processing tools are general enough to adapt to many types of irregular data [3].

Graph filterbanks with downsampling operations, be they critically sampled or oversampled, have often been defined

for signals defined on bipartite graphs because: i) Bipartite graphs, by definition, contain two sets of nodes that are natural candidates for the sampling operations on the nodes; ii) The combined operators downsampling followed by upsampling (which, concretely, forces to zero the graph signal on one of the two sets of nodes) may be exactly written as a filter in the graph Fourier space. This enables to write exact anti-aliasing equations for the low-pass and high-pass filters to control the spectral folding phenomenon due to sampling [15]. To apply these graph filterbanks to any arbitrary graph, one first needs to decompose the graph in a non-unique sum of bipartite graphs, and analyze each of them separately. Then, one usually iterates the filtering-downsampling operations on the approximation signal to obtain a multi-resolution analysis of the signal.

In this article, we propose a significantly different way of defining filterbanks. Instead of trying to find an exact equivalent of both the decimation operator, noted hereafter (\downarrow), and the filtering operator C , we directly define the equivalent of the decimated filtering operator $L = (\downarrow)C$. We follow here the notations of [22], where L is not to be confused with the Laplacian operator of the graph, noted \mathcal{L} . Consider the 1-D straight-line graph where each node has two neighbors, and a partition of this graph in subgraphs of pairs of adjacent nodes. The classical Haar low-pass (resp. high-pass) channel samples one node per subgraph and defines on it the local average (resp. difference) of the signal. By analogy, we will consider a partition of the graph in connected subgraphs, not necessarily of same size. We constrain the low-pass channel (resp. high-pass channels) to create one “supernode” per subgraph and define on it the local, i.e., over the subgraph, average (resp. differences) of the signal. The coarsened graph structures on which those downsampled signals are defined, are then derived from the connectivity between the subgraphs: two supernodes are linked if there are edges between the associated subgraphs.

With this method, we design a critically-sampled and orthogonal transform that is valid for any partition in connected subgraphs. Depending on the application at hand, one may choose one or another way of detecting such partitions. For the image approximation and denoising experiments presented here, a natural way of doing so is by detecting a partition in communities, i.e. groups of nodes more connected with themselves than with the rest of the network [23]. This community structure is indeed closely linked to the low frequencies of a signal, as one can see by plotting the first few graph Fourier modes (see for instance [20]). In fact, spectral graph clustering has been a historic way of detecting communities in a graph.

The article is organized as follows. Section II recalls the definition of the graph Fourier transform used here. In Section III, we introduce the main difficulty to extend filterbanks to graph signals, after a brief recall of the classical Haar filterbank, and we discuss the state-of-the-art of graph filterbanks. We

The authors are with the Laboratoire de Physique, CNRS, ENS de Lyon, Université de Lyon, F69007 Lyon, France (e-mail: firstname.lastname@ens-lyon.fr). Work supported by the ANR-14-CE27-0001 GRAPHSIP grant.

expose our contributions in Section IV where we first give intuition about the design via an analogy to the Haar filterbank, before presenting the new graph filterbank design. Section V discusses how to obtain a partition in connected subgraph. Section VI shows applications, in compression and denoising. We conclude in Section VII.

II. THE GRAPH FOURIER TRANSFORM

Let $\mathcal{G} = (\mathcal{V}, \mathcal{E}, \mathbf{A})$ be a undirected weighted graph with \mathcal{V} the set of nodes, \mathcal{E} the set of edges, and \mathbf{A} the weighted adjacency matrix such that $\mathbf{A}_{ij} = \mathbf{A}_{ji} \geq 0$ is the weight of the edge between nodes i and j . Note N the total number of nodes. Let us define the graph's Laplacian matrix $\mathcal{L} = \mathbf{D} - \mathbf{A}$ where \mathbf{D} is a diagonal matrix with $\mathbf{D}_{ii} = \mathbf{d}_i = \sum_{j \neq i} \mathbf{A}_{ij}$ the strength of node i . \mathcal{L} is real symmetric, therefore diagonalizable: its spectrum is composed of $(\lambda_l)_{l=1 \dots N}$ its set of eigenvalues that we sort: $0 = \lambda_1 \leq \lambda_2 \leq \lambda_3 \leq \dots \leq \lambda_N$; and of \mathbf{Q} the matrix of its normalized eigenvectors: $\mathbf{Q} = (\mathbf{q}_1 | \mathbf{q}_2 | \dots | \mathbf{q}_N)$. Considering only connected graphs, the multiplicity of eigenvalue $\lambda_1 = 0$ is 1 [24]. By analogy to the continuous Laplacian operator whose eigenfunctions are the continuous Fourier modes and eigenvalues their squared frequencies, \mathbf{Q} is considered as the matrix of the graph's Fourier modes, and $(\sqrt{\lambda_l})_{l=1 \dots N}$ its set of associated "frequencies" [2]. For instance, the graph Fourier transform $\hat{\mathbf{x}}$ of a signal \mathbf{x} defined on the nodes of the graph reads: $\hat{\mathbf{x}} = \mathbf{Q}^\top \mathbf{x}$.

III. STATE OF THE ART

A. The classical Haar filterbank for 1-D signals

The classical Haar filterbank will be used as a leading example to expose the main issues encountered when attempting to extend filterbanks to graph signals.

Consider the 1-D discrete signal \mathbf{x} of size N , and the decimation operator $(\downarrow 2)$ by 2, which keeps only one every two nodes. Let us recall that, at the first level of the classical Haar filterbank, \mathbf{x} is decomposed into [22]:

- its approximation \mathbf{x}_1 of size $N/2$:

$$\mathbf{x}_1 = (\downarrow 2)\mathbf{C}\mathbf{x}, \quad (1)$$

where \mathbf{C} is the sliding average operator, here in matrix form:

$$\mathbf{C} = \frac{1}{\sqrt{2}} \begin{bmatrix} 1 & 1 & 0 & 0 & \dots \\ 0 & 1 & 1 & 0 & \dots \\ 0 & 0 & 1 & 1 & \dots \\ \vdots & \vdots & \vdots & \vdots & \ddots \end{bmatrix}. \quad (2)$$

- and its detail \mathbf{x}_2 of size $N/2$:

$$\mathbf{x}_2 = (\downarrow 2)\mathbf{D}\mathbf{x}, \quad (3)$$

where \mathbf{D} is the sliding difference operator:

$$\mathbf{D} = \frac{1}{\sqrt{2}} \begin{bmatrix} -1 & 1 & 0 & 0 & \dots \\ 0 & -1 & 1 & 0 & \dots \\ 0 & 0 & -1 & 1 & \dots \\ \vdots & \vdots & \vdots & \vdots & \ddots \end{bmatrix}. \quad (4)$$

This Haar filterbank is said to be:
i) *orthogonal*. Indeed, the operator $\begin{bmatrix} (\downarrow 2)\mathbf{C} \\ (\downarrow 2)\mathbf{D} \end{bmatrix}$ is orthonormal: the inverse is its transpose. To recover \mathbf{x} from its approximation and detail, one only needs to compute:

$$\begin{aligned} & [((\downarrow 2)\mathbf{C})^\top \quad ((\downarrow 2)\mathbf{D})^\top] \begin{bmatrix} \mathbf{x}_1 \\ \mathbf{x}_2 \end{bmatrix} \\ &= [\mathbf{C}^\top (\uparrow 2) \quad \mathbf{D}^\top (\uparrow 2)] \begin{bmatrix} \mathbf{x}_1 \\ \mathbf{x}_2 \end{bmatrix} \\ &= [\mathbf{C}^\top (\uparrow 2) \quad \mathbf{D}^\top (\uparrow 2)] \begin{bmatrix} (\downarrow 2)\mathbf{C} \\ (\downarrow 2)\mathbf{D} \end{bmatrix} \mathbf{x} = \mathbf{x}, \end{aligned} \quad (5)$$

where $(\uparrow 2)$ is the upsampling operator.

ii) *critically sampled*. Indeed, the amount of post-filter information \mathbf{x}_1 and \mathbf{x}_2 (two vectors of size $N/2$ each) is equal to the amount of pre-filter information \mathbf{x} (of size N).

This highlights the central role of decimation $(\downarrow 2)$, which follows what we will call in the following the "one every two nodes paradigm". It also highlights what is needed to design a filterbank: 1) a decimation operator 2) a low-pass filter \mathbf{C} and a high-pass filter \mathbf{D} that combine well with each other and the decimation operator such that perfect recovery is possible.

B. Adapting filterbanks to graph signals

1) *The difficulty*: When designing filterbanks for graph signals, a key difficulty is the design of a suited decimation operator, and it comes in two separate problems :

i) how to choose the nodes to keep?

ii) how to wire together the nodes that are kept, so as to create the downsampled graph?

On a straight line or regular grids, issue i) is solved by the one every two nodes paradigm and issue ii) does not exist as the structure on which the downsampled signals are hence defined are exactly the same than the original structure: when downsampling a straight line (resp. 2D grid, ...), one obtains two straight lines (2D grids, ...); as shown in Fig. 1 a) and b).

In the case of arbitrary graphs, to tackle issue i), all contributing authors' visions (cited underneath in this section) boil down to find a way to adapt the one every two nodes paradigm to arbitrary graphs. As for issue ii): unlike regular grids, downsampling an arbitrary graph will almost always create graphs that do not share the same structural properties than the original, requiring specific node-wiring schemes.

We specifically recall in Section III-B2 Narang et al.'s [15], [25] proposition to these two issues, and in Section III-B3 Schuman et al.'s [26] proposition. This will enable us to clearly propose and situate our contribution in Section IV.

2) *A design for signals defined on bipartite graphs*: Narang and Ortega [15], [25] propose to consider signals defined on bipartite graphs (i.e. two-colourable graphs). In fact, in this particular case, one may still downsample the graph by naturally keeping one every two nodes, as shown in Fig. 1c). Then, the authors proposed the following wiring rule for the downsampled structures: two nodes are linked if they have at least a common neighbour in the initial graph (this scheme

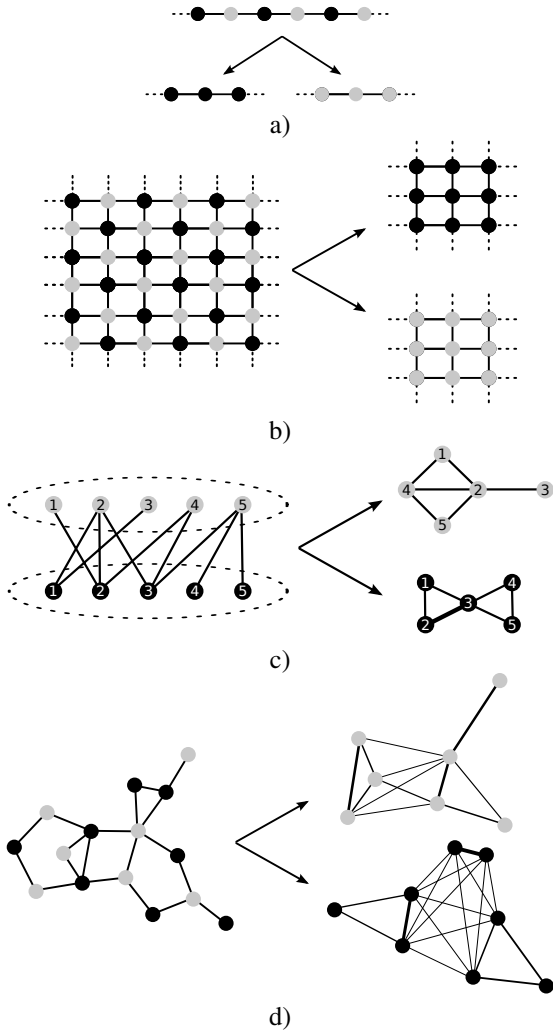


Fig. 1. Some state-of-the-art graph downsampling procedure, where the nodes are separated in two sets: the black and the gray nodes. They all follow the “one every two nodes” paradigm, with specific rules to define the two sets and to wire together the nodes after downsampling: a) (resp. b) follows the classical 1D (resp. 2D) downsampling example. For these regular graphs, the wiring simply follows the original graph’s regularity; In c), a bipartite graph is downsampling and wired following [15]; In d), two sets of nodes of an arbitrary graph are chosen according to the polarity of the highest frequency graph Fourier mode and each set is wired based on the Kron reduction [26].

is sometimes improved by assigning a weight to each link depending on the number of common neighbours). As seen in Fig. 1c), a downsampled bipartite graph is not necessarily bipartite. In order to iterate such a filterbank design, and also to make it applicable to any kind of original graph, the authors propose a pre-processing step of the structure where the initial graph is decomposed in a sum of bipartite subgraphs, on which the filterbank is successively applied. Other methods to create bipartite graphs have been recently proposed, for instance Sakiyama and Tanaka’s oversampling method [16], or Nguyen and Do’s maximum spanning tree method [17].

One of the desirable properties of this design is the specific behavior of bipartite graphs Laplacian’s eigenvalues, that enable the authors to write specific anti-aliasing equations for the design of the filters C and D (see Eq. (13) of [15]).

3) *A downsampling based on the Laplacian’s last eigenvector*: Another way of downsampling an arbitrary graph has been proposed by Shuman et al. [26]. The authors focus on the eigenvector associated to the Laplacian’s largest eigenvalue. More specifically, they create two sets of nodes depending on this eigenvector’s sign. According to the Fourier interpretation of the Laplacian’s eigenbasis, the last eigenvector corresponds to the “highest frequency” of a signal defined on the graph. This generalisation is appealing in that for structured grids and bipartite graphs, the sign of this eigenvector does alternate every two nodes. Graph coloring using eigenvalue decomposition is not a novel idea [27] but Shuman et al. are the first to use it for graph filterbanks.

Once one has two sets of nodes, the question then arises as to how each set should be wired to form two separate graphs. The authors in [26] rely on the Kron reduction [28] of the graph. This method is illustrated in Fig. 1d), where the black nodes correspond to negative eigenvector values, and gray nodes correspond to positive eigenvector values. The authors also propose a post-processing procedure where they remove links from otherwise very dense downsampled graphs (as far as graph signal processing is concerned, sparsity of the underlying structures is a desired property for computational efficiency), implying some degree of arbitrary choices.

IV. FILTERBANKS ON CONNECTED SUBGRAPHS

The path explored in this work lets go of the “one every two nodes” sampling paradigm, and rather concentrates on coarsening the structure by defining “supernodes” as representatives of entire connected subgraphs of the network. We will not, as in the quoted works, attempt to define separate analogies for graph signals, of the downsampling operators ($\downarrow 2$) and of the filter operators C and D . Instead we directly define an analogy to graph signals of the decimated sliding average operator:

$$L = (\downarrow 2)C = \frac{1}{\sqrt{2}} \begin{bmatrix} 1 & 1 & 0 & 0 & 0 & 0 & \dots \\ 0 & 0 & 1 & 1 & 0 & 0 & \dots \\ 0 & 0 & 0 & 0 & 1 & 1 & \dots \\ \vdots & \vdots & \vdots & \vdots & \vdots & \vdots & \ddots \end{bmatrix}, \quad (6)$$

and of the decimated sliding difference operator:

$$B = (\downarrow 2)D = \frac{1}{\sqrt{2}} \begin{bmatrix} -1 & 1 & 0 & 0 & 0 & 0 & \dots \\ 0 & 0 & -1 & 1 & 0 & 0 & \dots \\ 0 & 0 & 0 & 0 & -1 & 1 & \dots \\ \vdots & \vdots & \vdots & \vdots & \vdots & \vdots & \ddots \end{bmatrix}. \quad (7)$$

In Section IV-A, we first take a close look at the effect of the two classical operators L and B on the input signal x , to give insight in the fundamental analogy that is further formalized in Section IV-B. Our actual filterbank scheme is defined in Section IV-C. In Section IV-D, Haar filterbank is looked at as a particular case of our subgraph-based filterbanks.

A. Introducing the design by analogy to the Haar filterbank

We rephrase the classical Haar filterbank from a new point of view, different from the one adopted in Section III-A.

1) *Replace decimation by partition*: Consider the 1-D classical signal \mathbf{x} of size N defined on the straight line graph \mathcal{G} , of size N , where each node has two neighbors. Given this graph, we consider the partition \mathcal{c} of the graph in $K = N/2$ connected subgraphs $\{\mathcal{G}^k\}_{k \in \{1, K\}}$ connecting neighbors two-by-two: we call it the Haar partition, and it reads (when coded as a vector):

$$\mathbf{c}^\top = (1, 1, 2, 2, 3, 3, \dots), \quad (8)$$

where $\mathcal{c}(i)$ is the label of node i 's subgraph.

2) *Interpret operators \mathbf{L} and \mathbf{B} in term of local Fourier modes*: Consider subgraph \mathcal{G}^k and \mathbf{x}^k the restriction of \mathbf{x} to this subgraph. Define \mathcal{G}^k 's local adjacency matrix A^k :

$$\forall k \in \{1, N/2\} \quad A^k = \begin{bmatrix} 0 & 1 \\ 1 & 0 \end{bmatrix}. \quad (9)$$

Its associated Laplacian matrix is diagonalisable with two local Fourier modes:

$$\mathbf{q}_1^\top = \frac{1}{\sqrt{2}} (1, \quad 1) \quad (10)$$

of associated to eigenvalue $\lambda_1 = 0$ and

$$\mathbf{q}_2^\top = \frac{1}{\sqrt{2}} (1, \quad -1) \quad (11)$$

of associated to eigenvalue $\lambda_2 = 2$.

The actual effect of the operation $\mathbf{x}_1 = \mathbf{L}\mathbf{x}$ in Haar filterbank is to assign to each subgraph \mathcal{G}^k the first local Fourier component of \mathbf{x}^k :

$$\forall k \in \{1, \dots, N/2\} \quad \mathbf{x}_1(k) = \mathbf{q}_1^\top \mathbf{x}^k. \quad (12)$$

Similarly, the actual effect of the operation $\mathbf{x}_2 = \mathbf{B}\mathbf{x}$ may be rewritten as :

$$\forall k \in \{1, \dots, N/2\} \quad \mathbf{x}_2(k) = \mathbf{q}_2^\top \mathbf{x}^k. \quad (13)$$

In other words $[\mathbf{x}_1(k) \quad \mathbf{x}_2(k)]^\top$ is the local (reduced to \mathcal{G}^k) Fourier transform of \mathbf{x}^k .

3) *Analogy for graph signals*: Consider an arbitrary graph \mathcal{G} and an arbitrary partition \mathcal{c} of this graph in K connected subgraphs $\{\mathcal{G}^k\}_{k \in \{1, K\}}$. Consider one of these subgraphs \mathcal{G}^k of size N_k . The fundamental analogy we propose here is the following: consider the k -th component of the approximation and all detail signals $[\mathbf{x}_1(k) \quad \mathbf{x}_2(k) \quad \dots \quad \mathbf{x}_{N_k}(k)]^\top$ as the local graph Fourier transform of \mathbf{x}^k , the graph signal reduced to \mathcal{G}^k . To this end, we diagonalize \mathcal{G}^k 's local Laplacian matrix to find its N_k eigenvectors (a.k.a. local Fourier modes) sorted w.r.t. their eigenvalues (a.k.a. local Fourier square frequencies), and compute the successive inner products.

Note that, unlike the case of the straight line graph combined to Haar partition, all subgraphs will not necessarily be isomorph, nor of same size. In particular, this implies that only subgraphs of size at least l (i.e. only subgraphs for which there exist an l -th local Fourier mode) will contribute to \mathbf{x}_l . For instance, if a subgraph \mathcal{G}^k is reduced to a unique node, then its associated local Laplacian will only have one eigenvector: this particular subgraph will only contribute to $\mathbf{x}_1(k)$ and not to the detail signals $\{\mathbf{x}_l\}_{l \geq 2}$. On the other hand, if a subgraph \mathcal{G}^k contains three nodes, its local Laplacian will have three eigenvectors (sorted w.r.t. their eigenvalues). Its first

(resp. second, third) eigenvector will contribute to $\mathbf{x}_1(k)$ (resp. $\mathbf{x}_2(k)$, $\mathbf{x}_3(k)$). We develop the details in Section IV-B.

On which graphs are defined the downsampled signals? Having revisited the effects of operators \mathbf{L} and \mathbf{B} as a combination of local Fourier transforms, a question remains: on which graphs are defined the downsampled signals \mathbf{x}_1 , \mathbf{x}_2 , \mathbf{x}_3, \dots ? Consider an arbitrary graph \mathcal{G} and an arbitrary partition \mathcal{c} of this graph in K connected subgraphs $\{\mathcal{G}^k\}_{k \in \{1, K\}}$. Let us consider a supernode k for each subgraph \mathcal{G}^k , and define \mathcal{G}_l (of adjacency matrix \mathbf{A}_l) the graph on which \mathbf{x}_l is defined. For $l = 1$, $\mathbf{A}_1(k, k')$ is the sum of the weights of the links connecting subgraph k to subgraph k' in the original graph. For $k = k'$, and by convention, we impose no self-loop, i.e. $\mathbf{A}_1(k, k) = 0$. For the subsequent graphs \mathcal{G}_2 , \mathcal{G}_3 , \dots on which are defined \mathbf{x}_2 , \mathbf{x}_3 , \dots , we encounter the issue previously pointed that the subgraphs do not have the same size. Hence they do not all participate in the definition of \mathbf{x}_l . In fact, only subgraphs containing at least l nodes participate to the definition of \mathbf{x}_l . Therefore, to define \mathcal{G}_2 (resp. \mathcal{G}_3 , \mathcal{G}_4 , etc.), we first discard all subgraphs that contain strictly less than 2 (resp. 3, 4, etc.) nodes, and create the remaining subgraph connectivity matrix \mathbf{A}_2 (resp. \mathbf{A}_3 , \mathbf{A}_4 , etc.), on which \mathbf{x}_2 (resp. \mathbf{x}_3 , \mathbf{x}_4 , etc.) is defined. Details are developed in Section IV-B. In the case of a straight-line graphs \mathcal{G} and of Haar partition, \mathcal{G}_1 and \mathcal{G}_2 are also straight-line graphs of size $N/2$.

B. Definition of operators necessary to the design

1) *Subgraph indicator operators*: Consider an arbitrary graph \mathcal{G} and an arbitrary partition \mathcal{c} of this graph in K connected subgraphs $\{\mathcal{G}^k\}_{k \in \{1, \dots, K\}}$. Write N_k the number of nodes in subgraph \mathcal{G}^k of label k . Let us first define the matrix $\mathbf{S} \in \mathbb{R}^{N \times K}$, a more practical way (for linear algebra calculus) than vector \mathbf{c} to encode the connected subgraph structure :

$$\mathbf{S} = (\mathbb{1}_{\text{Csub } 1} | \mathbb{1}_{\text{Csub } 2} | \dots | \mathbb{1}_{\text{Csub } K}). \quad (14)$$

where $\mathbb{1}_{\text{Csub } k}$ is subgraph k 's indicator function, i.e.:

$$\begin{aligned} \mathbb{1}_{\text{Csub } k}(i) &= 1 \text{ if } \mathcal{c}(i) = k \\ &= 0 \text{ if not.} \end{aligned} \quad (15)$$

For each subgraph \mathcal{G}^k composed of N_k nodes $\{v_{\sigma^k(1)}, v_{\sigma^k(2)}, \dots, v_{\sigma^k(N_k)}\}$, let us define the sampling operator \mathbf{C}_k of size $N \times N_k$:

$$\mathbf{C}_k = (\boldsymbol{\delta}_{\sigma^k(1)} | \boldsymbol{\delta}_{\sigma^k(2)} | \dots | \boldsymbol{\delta}_{\sigma^k(N_k)}), \quad (16)$$

where $\boldsymbol{\delta}_{\sigma^k(i)}(j) = 1$ if $\sigma^k(i) = j$, and zero otherwise.

2) *Subgraph Laplacian operators*: The adjacency matrix \mathbf{A} may be written as the sum of two adjacency matrices:

- the intra-subgraph adjacency matrix:

$$\mathbf{A}_i = \sum_{k=1}^K \mathbf{C}_k \mathbf{C}_k^\top \mathbf{A} \mathbf{C}_k \mathbf{C}_k^\top, \quad (17)$$

that keeps only the links within subgraphs.

- the inter-subgraph adjacency matrix $\mathbf{A}_e = \mathbf{A} - \mathbf{A}_i$ that keeps only the links connecting subgraphs together.

In the following, we note \mathbf{A}_i^k the reduction of \mathbf{A}_i to subgraph \mathcal{G}^k , i.e.:

$$\forall k \in \{1, \dots, K\} \quad \mathbf{A}_i^k = \mathbf{C}_k^\top \mathbf{A}_i \mathbf{C}_k, \quad (18)$$

and \mathcal{L}_i^k the local Laplacian associated to \mathbf{A}_i^k . In other words, \mathcal{L}_i^k is the Laplacian matrix of subgraph \mathcal{G}^k of size N_k . It is diagonalisable:

$$\forall k \in \{1, \dots, K\} \quad \mathcal{L}_i^k = \mathbf{Q}^k \mathbf{\Lambda}^k \mathbf{Q}^{k\top}, \quad (19)$$

with $\mathbf{\Lambda}^k$ the diagonal matrix of sorted eigenvalues (λ_1^k is the smallest):

$$\mathbf{\Lambda}^k = \text{diag}(\lambda_1^k, \lambda_2^k, \dots, \lambda_{N_k}^k), \quad (20)$$

and \mathbf{Q}^k the orthonormal basis of local Fourier modes:

$$\mathbf{Q}^k = (\mathbf{q}_1^k | \mathbf{q}_2^k | \dots | \mathbf{q}_{N_k}^k). \quad (21)$$

Furthermore, for each eigenvector \mathbf{q}_i^k of size N_k defined on the local subgraph \mathcal{G}^k , we note $\bar{\mathbf{q}}_i^k$ its zero-padded extension to the whole global graph:

$$\forall k \in \{1, K\} \quad \forall i \in \{1, N_k\} \quad \bar{\mathbf{q}}_i^k = \mathbf{C}_k \mathbf{q}_i^k. \quad (22)$$

Nota bene: we could have of course obtained the $\bar{\mathbf{q}}_i^k$ by direct diagonalization of the Laplacian matrix of \mathbf{A}_i , but we need the introduced notations for the next definitions.

3) *Fourier and Group operators:* Considering the connected subgraph partition \mathbf{c} , define \tilde{N}_1 the maximum number of nodes in any subgraph:

$$\tilde{N}_1 = \max_k N_k. \quad (23)$$

For any $l \in \{1, \dots, \tilde{N}_1\}$, we note I_l the list of subgraph labels containing at least l nodes:

$$\forall l \in \{1, \dots, \tilde{N}_1\} \quad I_l = \{k \in \{1, K\} \text{ s.t } N_k \geq l\}. \quad (24)$$

For instance, as all subgraphs contain at least 1 node, I_1 contains all the K subgraph labels. Also, necessarily: $|I_1| \geq |I_2| \geq \dots \geq |I_K|$ (where $|\cdot|$ denotes the cardinal).

The family of Fourier operators are the \tilde{N}_1 operators:

$$\forall l \in \{1, \dots, \tilde{N}_1\} \quad \mathbf{Q}_l = \left(\bar{\mathbf{q}}_l^{I_l(1)} | \bar{\mathbf{q}}_l^{I_l(2)} | \dots | \bar{\mathbf{q}}_l^{I_l(|I_l|)} \right). \quad (25)$$

This means that operator \mathbf{Q}_l groups together all local Fourier modes associated to the l -th eigenvalue of all subgraphs containing at least l nodes.

The family of Group operators also contains \tilde{N}_1 operators defined as, $\forall l \in \{1, \dots, \tilde{N}_1\}$:

$$\mathbf{S}_l = \left(\mathbb{1}_{\text{Csub } I_l(1)} | \mathbb{1}_{\text{Csub } I_l(2)} | \dots | \mathbb{1}_{\text{Csub } I_l(|I_l|)} \right). \quad (26)$$

This means that \mathbf{S}_l groups together indicator functions of subgraphs containing at least l nodes.

C. The filterbank design

1) *Analysis block:* Given a signal \mathbf{x} defined on the graph whose adjacency matrix is \mathbf{A} , one first needs to find a partition \mathbf{c} in connected subgraphs. The maximum number of nodes in any subgraph of \mathbf{c} is \tilde{N}_1 (see eq. (23)) and it determines the number of channels through which \mathbf{x} will be analyzed. Then, from \mathbf{c} , one constructs all operators \mathbf{Q}_l and \mathbf{S}_l as described in Section IV-B. Finally, the signal \mathbf{x} defined on the graph is decomposed, through the \tilde{N}_1 channels, in \tilde{N}_1 signals:

$$\forall l \in \{1, \dots, \tilde{N}_1\} \quad \mathbf{x}_l = \mathbf{Q}_l^\top \mathbf{x}, \quad (27)$$

each of them defined on a graph whose adjacency matrix reads:

$$\mathbf{A}_l = \mathbf{S}_l^\top \mathbf{A}_e \mathbf{S}_l. \quad (28)$$

2) *A remark on the storage of structural information:* An important question is whether the total amount of stored information pre- and post-analysis equal or not? In terms of signal information only (i.e., discarding the structural information), the total amount of stored information is equal on both sides of the analysis block as each of the downsampled signals \mathbf{x}_l is of size $|I_l|$ and $\sum_l |I_l| = N$.

On the other hand, in terms of structural information (i.e. the information of the adjacency matrices), one needs to keep both the structural information pre- and post-analysis. Indeed, the post-analysis structural information is not enough to reconstruct the original graph (unlike the signal \mathbf{x} who can be perfectly reconstructed from its approximation and details, as we will see in Section IV-C3). The amount of stored structural information therefore increases after analysis and this is –at least for now– an irreducible storage price to pay. This is a common downfall of all graph filterbanks yet proposed, e.g. [15]–[17], [25], [26]. Finding ways to critically sample both the structure and the signal defined on it is part of our ongoing research and is not in the scope of this article.

In the following, all graph structures are stored in the form $\mathbf{A} = \mathbf{A}_i + \mathbf{A}_e$, as this does not increase the amount of information (the number of links) but still subtly encodes the connected subgraph structure: indeed the partition \mathbf{c} can be exactly recovered by detecting the connected components of \mathbf{A}_i . In Narang et al. [15], [25], authors also need to keep an information equivalent to \mathbf{c} : the bipartite graph decomposition of \mathbf{A} and, for each bipartite graph, the information of the two sets of nodes. It is also the case in Shuman et al. [26]’s work, where authors need to keep the downsampling vector \mathbf{m} .

3) *Synthesis block:* Let us show that storing only $\{\mathbf{x}_l\}_{l \in \{1, \dots, \tilde{N}_1\}}$ is enough to perfectly recover \mathbf{x} . In fact, from the knowledge of the subgraph structure \mathbf{c} extracted from \mathbf{A}_i , one obtains $\{\mathbf{Q}_l\}_{l \in \{1, \dots, \tilde{N}_1\}}$ from the computations of Sections IV-B2 and IV-B3. It follows that \mathbf{x} is perfectly recovered by computing :

$$\tilde{\mathbf{x}} = \sum_{l=1}^{\tilde{N}_1} \mathbf{Q}_l \mathbf{x}_l = \sum_{l=1}^{\tilde{N}_1} \mathbf{Q}_l \mathbf{Q}_l^\top \mathbf{x} = \mathbf{x}. \quad (29)$$

We show in Fig. 2 a schematic representation of the analysis and synthesis blocks of the proposed graph filterbanks.

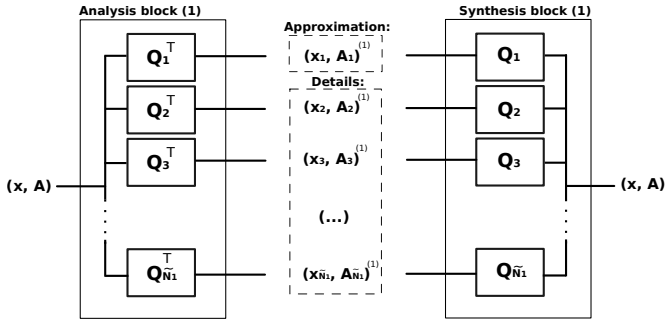


Fig. 2. Schematic representation of the analysis and synthesis blocks of the proposed filterbanks.

4) *Critical sampling and orthogonality*: Starting with data \mathbf{x} of size N , the analysis block provide vectors \mathbf{x}_l of size $|I_l| \forall l \in \{1, \dots, \tilde{N}_1\}$. Storing all the \mathbf{x}_l accounts for $\sum_l |I_l| = N$ values: the filterbank is critically sampled.

Furthermore, this filterbank is orthogonal. Indeed, the analysis filter combining the \tilde{N}_1 channels may be written as $[Q_1 \ Q_2 \ \dots \ Q_{\tilde{N}_1}]^\top$. This filter is, by construction, orthonormal and its inverse is its transpose:

$$[Q_1 \ Q_2 \ \dots \ Q_{\tilde{N}_1}] \begin{bmatrix} Q_1^\top \\ Q_2^\top \\ \dots \\ Q_{\tilde{N}_1}^\top \end{bmatrix} = I_N, \quad (30)$$

where I_N is the identity matrix of size N .

D. The classical Haar filterbank as a particular case of this subgraph-based filterbank design

Given the proposed design, we take a last look at the classical Haar filterbank to show it as a particular case.

In one dimension. Consider the straight-line graph on which a signal \mathbf{x} of size N is defined, and the Haar partition of this graph (eq. (8)). One has the following equivalences:

$$\tilde{N}_1 = 2, \quad L = Q_1^\top \quad \text{and} \quad B = Q_2^\top. \quad (31)$$

Moreover, $A_1 = A_2$ and code for straight-line graphs of size $N/2$.

In two dimensions. Consider the two dimensional regular grid graph of size $\sqrt{N} \times \sqrt{N}$, on which an image of size N is defined. In two dimensions, the Haar partition consists in separating the graph in “squares” of size 4. Also, the classical Haar classical filterbank contains 4 channels, that are naturally uncovered in our design ($\tilde{N}_1 = 4$) as the global analysis filter:

$$[Q_1 \ Q_2 \ Q_3 \ Q_4]^\top \quad (32)$$

Moreover, $A_1 = A_2 = A_3 = A_4$ all code for two dimensional regular grid graphs of size $\sqrt{N/4} \times \sqrt{N/4}$

E. The analysis cascade

Filterbanks are most useful when organised in cascade, each level of which contains the analysis and synthesis operators defined in Section IV-C. In fact, given an original graph of

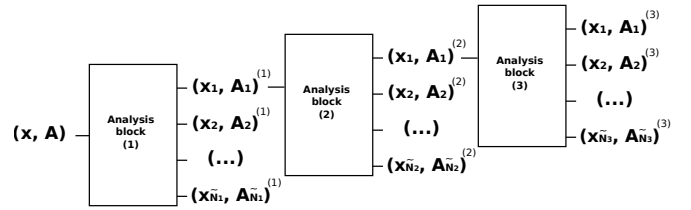


Fig. 3. The first three levels of the analysis cascade.

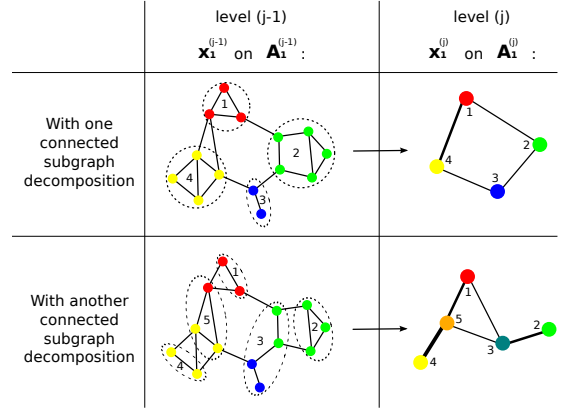


Fig. 4. Approximation $(\mathbf{x}_1^{(j)}, \mathbf{A}_1^{(j)})$ at level (j) of an analysis cascade of the signal-structure couple $(\mathbf{x}_1^{(j-1)}, \mathbf{A}_1^{(j-1)})$, given two different partitions in connected subgraphs (represented by the dotted lines). The signal is represented by colors on the nodes. Subgraph k in the original graph is represented by supernode k in the coarsened graph. As seen in Section IV, the signal on supernode k is the signal’s average on the original subgraph k . Note the strong impact of the partition on the approximation signal.

adjacency matrix \mathbf{A} , and a signal \mathbf{x} defined it, one obtains the \tilde{N}_1 channels of the first level of the cascade noted:

$$\left\{ (\mathbf{x}_l, \mathbf{A}_l)^{(1)} \right\}_{l \in \{1, \tilde{N}_1\}}. \quad (33)$$

For each of these channels, one may iterate the same analysis scheme, thereby obtaining successive approximations and details of the original signal at different scales of analysis. Classically, one iterates the analysis scheme only on the approximation signal at each level of the cascade, as shown on Fig. 3. Note that the number of channels is not necessarily constant down the cascade. It is in fact adaptative: the number of channels of the analysis block $(j+1)$ depends on the maximal number of nodes \tilde{N}_j contained in the subgraphs defined by the partition $c^{(j)}$.

V. DETECTING A PARTITION OF CONNECTED SUBGRAPHS

The proposed filterbank explicitly integrates the graph structure in connected subgraphs. A central question arises: how does one choose a particular partition c of the graph in connected subgraphs? This choice of partition has a strong influence on what the filterbanks achieve, as shown in Fig. 4 where we compare the effect of downsampling for two different partitions on a toy graph. The practitioner has the choice among a wide variety of options to find such a partition: he could follow graph partitioning techniques of [29] or [30], or use graph nodal domains [31] – either very high frequency ones as in [26] or others — or any other solution... While the

proposed filterbanks is well-defined for any of these partitions, the final decision regarding the partitioning algorithm will depend on what the user wants the filterbanks to achieve.

In the following, we show applications for compression and denoising. Therefore we seek a design that typically transforms the original signal in a sparser one after analysis. For that, we decide to look for partitions that separate the graph into groups of nodes more connected to themselves than with the rest of the graph (also known as communities). Indeed, as in image or video compression, we suppose that low-frequencies contain in general the useful information of the signal. Approximating a community of nodes, each having its signal value, by a supernode on which we define the average of the signal over the community is a natural way of keeping the signal's low-frequencies.

Literature is abundant about community detection (see the survey [23]). Here, we detect non-overlapping communities using the greedy Louvain method [32] for maximizing the so-called modularity, a well-known objective function that measures the quality of a partition in communities. The Louvain method iteratively repeats two main phases: 1) From an initial situation where there is one community per node, each node is individually moved to another community until no individual move can improve the modularity; 2) The aggregation of each community in a “supernode” and the building a new adjacency matrix of this “supernode” graph. Phase 1 is then applied to this new graph, and so on and so forth. The algorithm stops when the modularity at the end of a phase 1 is not larger than the modularity obtained at the end of the previous phase 1. Iterating these two phases, communities become gradually larger. In our implementation, we impose a supplementary stopping criterion: the algorithm is stopped (if not already stopped thanks to the first criterion) as soon as the size of the largest community is larger than a given threshold τ . Indeed, to compute the local Fourier bases associated to each community, one needs to diagonalize Laplacian matrices: in order to keep computation time under control, we do not allow communities larger than the threshold, hereafter $\tau = 1000$ nodes.

Let us define two different types of filterbanks:

- **CoSub**, short for Connected Subgraphs Filterbanks, based on applying the Louvain algorithm on the adjacency matrix \mathbf{A} to be able to write $\mathbf{A} = \mathbf{A}_i + \mathbf{A}_e$;
- **EdAwCoSub**, short for Edge Aware Connected Subgraphs Filterbanks, taking the signal \mathbf{x} into account to modify the adjacency matrix into

$$\mathbf{A}_x(i, j) = \begin{cases} e^{-\frac{(\mathbf{x}(i) - \mathbf{x}(j))^2}{2\sigma_x^2}} & \text{if } \mathbf{A}(i, j) \neq 0 \\ 0 & \text{if } \mathbf{A}(i, j) = 0 \end{cases} \quad (34)$$

where $\sigma_x = \text{std}(\{\mathbf{x}(i) - \mathbf{x}(j)\}_{i \sim j})$ ($i \sim j$ means i neighbor to j in \mathbf{A}). The Louvain algorithm is then applied on \mathbf{A}_x . The obtained partition enables us to decompose the original adjacency matrix in $\mathbf{A} = \mathbf{A}_i + \mathbf{A}_e$.

Edge-awareness could also be implemented, as in [21], by adapting classical image segmentation methods to graph signals; we will keep a precise comparison between edge-awareness methods for future work.

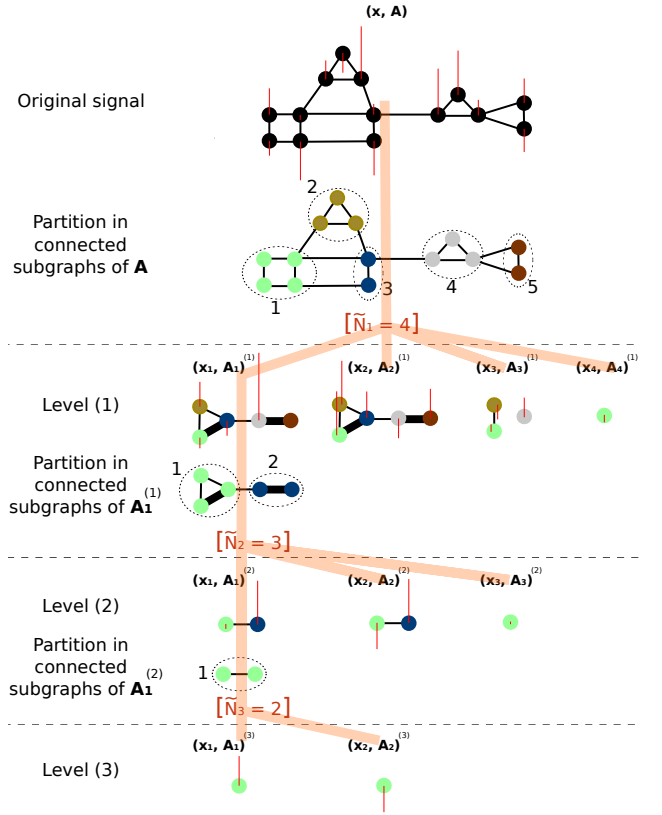


Fig. 5. An analysis cascade of a signal \mathbf{x} defined on a toy graph \mathbf{A} (top figure). On each node, the red vertical bar is proportional to the value of this node's signal. Each edge's width is proportional to its weight. Under the top figure is represented a partition in connected subgraph (see Section V); for clarity's sake, one color is assigned to each subgraph. The largest subgraph contains $\tilde{N}_1 = 4$ nodes: the first level of the cascade therefore contains $\tilde{N}_1 = 4$ channels. At level (1), we represent the approximation $(\mathbf{x}_1, \mathbf{A}_1)^{(1)}$ and the three details $\{(\mathbf{x}_l, \mathbf{A}_l)^{(1)}\}_{l=2,3,4}$. For each of the coarsened graphs, the color of each supernode corresponds to the color of \mathbf{A} 's subgraph it represents. We then iterate the analysis on the successive approximation signals, until level (3), where the approximation signal $(\mathbf{x}_1, \mathbf{A}_1)^{(3)}$ is reduced to a single node. The underlying orange tree is a guide to the eye down the analysis cascade. From the 6 detail and 1 approximation signals of each of its leaves, one may perfectly recover the original signal \mathbf{x} .

VI. APPLICATIONS

A. Two illustrative examples

1) *A signal defined on a simple toy graph:* Let us start by showing an analysis cascade on a toy signal defined on a very simple graph. We consider a 14 node graph and a signal defined on it as shown on the top of Fig. 5. The rest of Fig. 5 illustrates the analysis cascade of this graph signal.

For instance, let us take a close look at subgraph with label 5 of the original graph: it contains two nodes and the signal on each of its node is of same absolute value but of opposite signs. As expected, $\mathbf{x}_1^{(1)}(5)$, the approximation signal on the corresponding supernode at level (1) is null: it is the normalized sum of the two original values; and $\mathbf{x}_2^{(1)}(5)$, the first detail signal is large: it is the normalized difference between the two original values. Moreover, as this subgraph contains only 2 nodes, its Laplacian does not have a third eigenvector: this subgraph does not participate to the second and third detail signals and its associated supernode does not

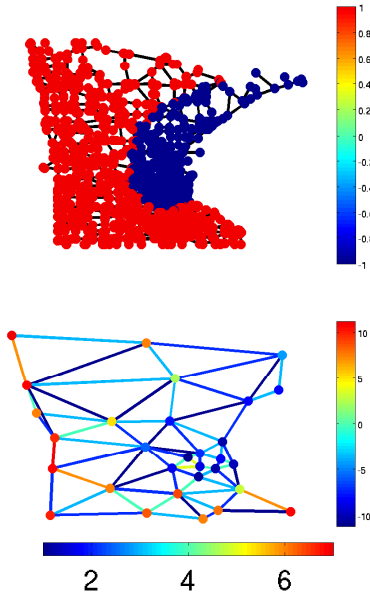


Fig. 6. Original (top) and approximated (bottom) piece-wise constant graph signal defined on the Minnesota traffic graph. Colorbars on the right of each figure corresponds to the values of the signal on each node. The colorbar on the bottom of the approximated graph corresponds to the weights of the links of the coarsened graph. The original graph is binary and therefore does not need such a colorbar.

appear in $(x_3, A_3)^{(1)}$ nor $(x_4, A_4)^{(1)}$.

The analysis cascade decomposes the original signal in 3 detail signals (of sizes 5, 3 and 1) at level (1), 2 detail signals (of sizes 2 and 1) at level (2), 1 detail signal and one approximation signal (both of size 1) at level (3). From these 7 downsampled signals of total size 14, one may perfectly reconstruct the original signal, using the synthesis operators defined in Section IV-C3.

2) *An example of approximated graph signal:* Fig. 6 (top) shows a piece-wise constant graph signal defined on the Minnesota traffic graph [25], and (bottom) the approximated signal $(x_1, A_1)^{(1)}$ after one level of analysis.

B. Reconstruction of images using non-linear approximation

Classical filterbanks have been widely used in image processing for many purposes including compression. Interestingly, images may be considered as graph signals defined on the two-dimensional regular grid (each pixel is a node, and each node has four neighbours), and may therefore be analyzed with graph-based filterbank approaches. We study here, in terms of quality of the reconstruction after compression, what the proposed design achieve, and it is in general as good as other classical or graph-based filterbanks.

Consider square images of size $\sqrt{N} \times \sqrt{N}$, therefore consisting of a signal of size N on a graph with N nodes. Consider for instance the benchmark image *cameraman* shown in Fig. 7 (top left). Its size is 256×256 ($N = 65536$). After a three-level decomposition of a classical filterbank, and keeping 3% of the high-pass coefficients, one reconstructs

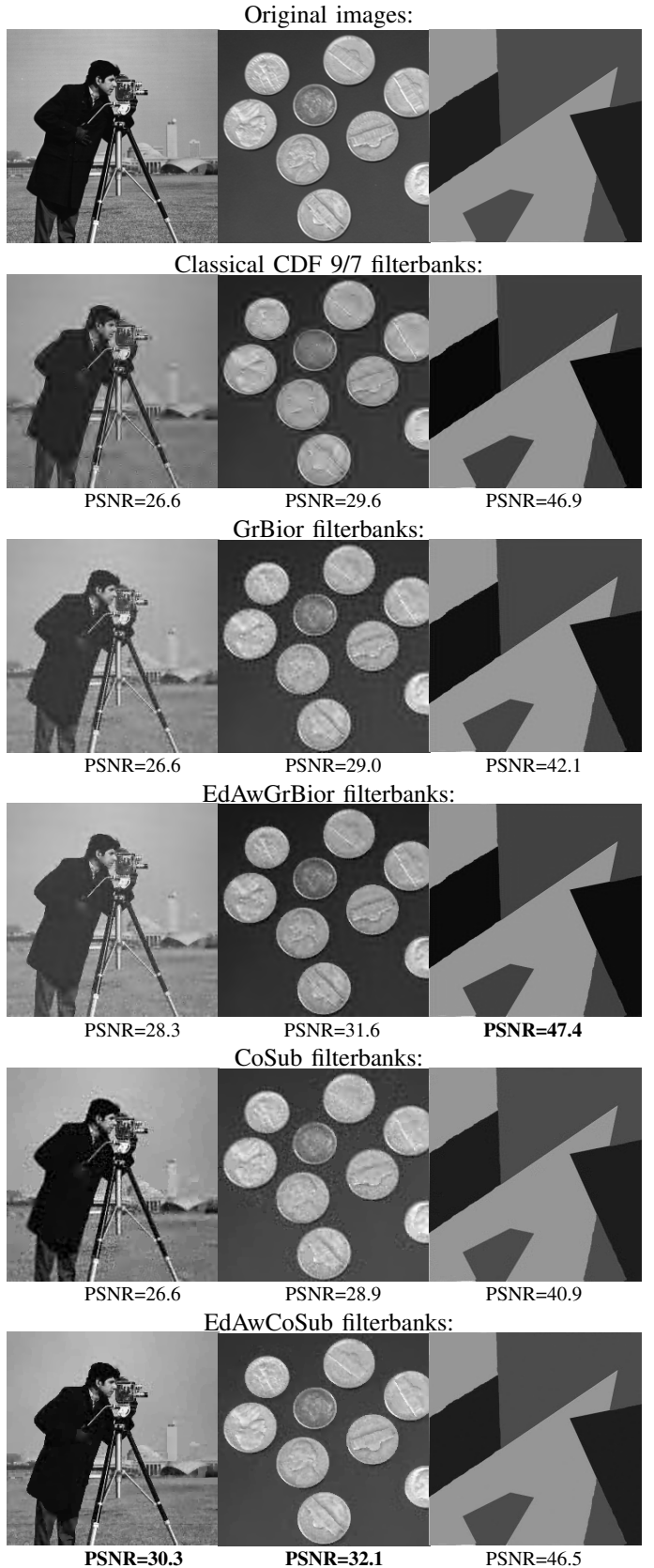


Fig. 7. Comparison, using different filterbank methods, of reconstructed images keeping 3% of the high-pass coefficients on three benchmark images. See Section VI-B for details.

% HP coef	0	1	2	3	4	8	16
<i>Synthetic</i>							
CDF 9/7	30.4	37.9	42.8	46.9	50.6	66.4	107
GrBior	30.5	36.2	39.4	42.1	44.7	54.9	71.7
EdAwGrBior	33.7	41.2	44.7	47.4	50.0	59.4	75.5
CoSub	35.1	37.5	39.3	40.9	42.3	47.7	59.9
EdAwCoSub	33.9	40.6	44.0	46.5	48.7	57.3	93.6
<i>Cameraman</i>							
CDF 9/7	20.7	23.3	25.2	26.6	27.5	30.7	35.6
GrBior	20.7	23.9	25.4	26.6	27.5	30.6	35.3
EdAwGrBior	21.4	25.7	27.2	28.3	29.2	32.1	36.7
CoSub	23.1	24.6	25.6	26.6	27.4	29.9	33.9
EdAwCoSub	27.4	28.7	29.6	30.3	31.0	33.2	37.0
<i>Coins</i>							
CDF 9/7	23.3	26.4	28.2	29.6	30.7	34.2	40.0
GrBior	23.3	26.1	27.8	29.0	30.1	33.6	38.9
EdAwGrBior	25.8	28.9	30.5	31.6	32.6	35.7	40.5
CoSub	25.1	26.7	27.9	28.9	29.8	32.8	37.5
EdAwCoSub	29.5	30.6	31.4	32.1	32.8	34.9	38.4

TABLE I

PSNR VERSUS THE PERCENTAGE OF HIGH-PASS COEFFICIENTS, FOR DIFFERENT FILTERBANK METHODS, ON THREE BENCHMARK IMAGES.

the image from $65536/64 = 1024$ low-pass coefficients and $0.03 * (65536 - 1024) = 1935$ high-pass coefficients, hence a total of 2959 coefficients (instead of the 65536 values of the original signal). In our design, because we do not use the one every two nodes paradigm, the size of the approximated signal decreases faster down our analysis cascade and we will often find an approximation with less than 1024 points well before the third level. In the case of the *cameraman* image, after the automatic connected subgraph decomposition (following Section V), one finds $K = 546$ subgraphs: the approximation signal $x_1^{(1)}$ is therefore already of size inferior to 1024 at level (1). Therefore, we stop the cascade at its first iteration, keeping the approximation signal of size 546 and 3.71% of the high-pass coefficients – in order to have exactly the same number of 2959 non-zero coefficients before reconstruction.

We compare in Fig. 7 (left column) the reconstructed image after several filterbanks: a classical one (CDF 9/7); a Graph Bior filterbank [25] with Nonzero DC and *graphBior(6,6)* filters (GrBior); the same Graph Bior filterbank but including edge-awareness [21] (EdAwGrBior); and the new connected-subgraph filterbank scheme with (EdAwCoSub) and without (CoSub) edge-awareness. On the middle and right columns, the same comparison is shown for two other benchmark images: *coins* (of size 240×240) and *synthetic* (of size 424×424). Finally, Table I shows further reconstruction results if one keeps more –or less– high-pass coefficients.

In general, CDF 9/7, GrBior and CoSub behave similarly with a difference: the higher (resp. lower) the compression rate, the better is CoSub (resp. CDF 9/7) compared to the other two. GrBior, for all compression rates, shows a median performance. Moreover, in general, the two edge-aware filterbanks, without surprise, have a better performance than the other three; and the higher the compression rate, the better is EdAwCoSub compared to EdAwGrBior. For a fair comparison, note that CDF 9/7 does not necessitate to store the structure of the graph (and subsequent coarsened graphs), whereas all graph methods do; and this is not taken into account in these comparisons (see the discussion in Section IV-C2).

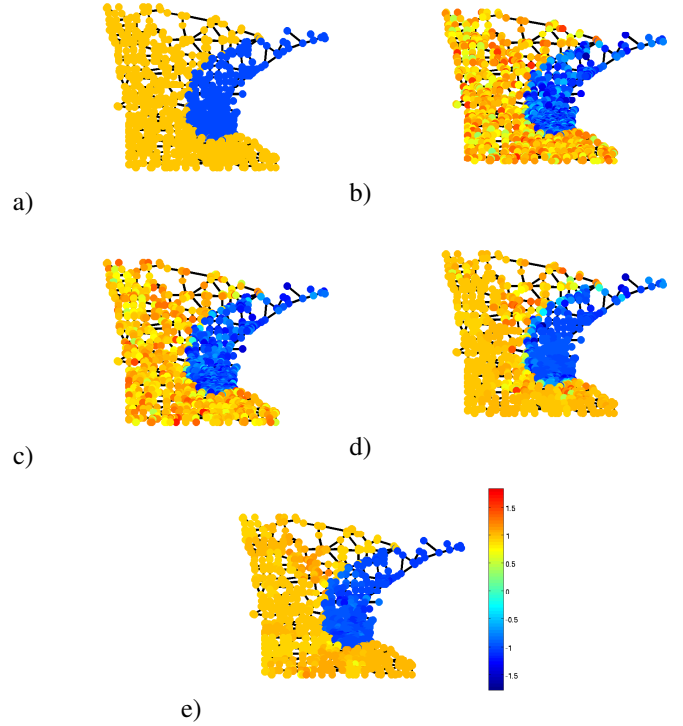


Fig. 8. a) Original piece-wise constant signal on the Minnesota traffic graph (the signal has only two values: ± 1), and b) its corrupted version with an additive Gaussian noise of standard deviation $\sigma = 1/4$. The three other figures are denoised signals after a one-level analysis and hard-thresholding all high-pass coefficients with $T = 3\sigma$. c) GrBior; d) CoSub; e) EdAwCoSub.

σ	noisy	GrBior	CoSub	EdAwCoSub
1/32	30.1	31.1	33.4	44.0
1/16	24.2	25.3	27.2	37.9
1/8	18.2	19.2	21.3	31.2
1/4	12.0	13.3	17.1	23.2
1/2	6.0	7.1	12.8	16.2
1	-0.1	1.2	8.9	8.9
2	-6.0	-4.7	4.9	2.9

TABLE II

SNR VERSUS σ IN THE DENOISING EXPERIMENT DETAILED IN SECTION VI-C.

Finally, these results can be compared with those obtained by Sakiyama et al. and summarized in Table 1 of [16]. In this work, the authors extend the edge-aware Graph Bior filterbanks and propose edge-aware Graph Bior filterbanks defined on oversampled Laplacian matrices. Their results are slightly better for *synthetic* and for low compression rates of *coins*.

C. Application in denoising, on the Minnesota traffic graph

Another usual application of filterbanks is denoising. We consider here a piece-wise constant graph signal (that has only two possible values: +1 and -1) defined on the Minnesota traffic graph, as shown in Fig. 8a. We corrupt this signal with an additive Gaussian noise of standard deviation σ . Fig. 8b

shows such a corrupted signal with $\sigma = 1/4$. We then attempt to recover the original image by:

- computing the first level of the analysis cascade,
- and reconstructing the signal from all low-pass coefficients and thresholded high-pass coefficients, having absolute value higher than $T = 3\sigma$.

Fig. 8c shows the result obtained with Graph Bior filterbanks. Fig 8d (resp. e) shows the result obtained with CoSub (resp. EdAwCoSub) filterbanks. Finally, Table II summarizes SNR results for different values of σ . Once again, this Table may also be completed by results obtained by Sakiyama et al. and summarized in Table 5 of [16]. Results are here univocal: our methods outperform existing ones. EdAwCoSub has a very high performance at low σ and loses progressively its advantage as σ increases: this is because edges in the signal become increasingly fuzzy as σ increases. Interestingly, CoSub performs better than GrBior for all σ , and better than Sakiyama et al.'s method for the three largest values of σ .

VII. CONCLUSION

An original framework for graph filterbanks is proposed in this work. Whereas all existing methods are based on the “one every two nodes” paradigm either through the sign of the highest frequency graph Fourier mode, or through bipartite graph decompositions, we coarsen the graph by defining supernodes representing its decomposition in connected subgraphs. Also, while previous methods are based on global filters defined in the global Fourier space of the graph, we define local filters based on the local Fourier spaces of each connected subgraph. Following this new paradigm, we design here the simplest form of filterbanks, that one could call Haar graph filterbank: the k -th value of the downsampled approximation (resp. details) is the average (resp. differences) of the signal on subgraph k . This simple idea shows at least state-of-the-art performances on usual benchmarks, and outperforms many methods in image compression at high compression rates, and in simple denoising experiments. Within this framework, future work will concentrate on extending the local filters to more sophisticated filters, and on finding ways to critically sample jointly the graph structure and the graph signal defined on it.

REFERENCES

- [1] M. Newman, *Networks: an introduction*. Oxford University Press, 2010.
- [2] D. Shuman, S. Narang, P. Frossard, A. Ortega, and P. Vandergheynst, “The emerging field of signal processing on graphs: Extending high-dimensional data analysis to networks and other irregular domains,” *Signal Processing Magazine, IEEE*, vol. 30, no. 3, pp. 83–98, May 2013.
- [3] A. Sandryhaila and J. Moura, “Big data analysis with signal processing on graphs: Representation and processing of massive data sets with irregular structure,” *Signal Processing Magazine, IEEE*, vol. 31, no. 5, pp. 80–90, Sept 2014.
- [4] D. Hammond, P. Vandergheynst, and R. Gribonval, “Wavelets on graphs via spectral graph theory,” *Applied and Computational Harmonic Analysis*, vol. 30, no. 2, pp. 129–150, 2011.
- [5] A. Sandryhaila and J. Moura, “Discrete signal processing on graphs,” *Signal Processing, IEEE Transactions on*, vol. 61, no. 7, pp. 1644–1656, April 2013.
- [6] —, “Discrete signal processing on graphs: Graph fourier transform,” in *Acoustics, Speech and Signal Processing (ICASSP), 2013 IEEE International Conference on*, May 2013, pp. 6167–6170.

- [7] S. Narang, A. Gadde, and A. Ortega, “Signal processing techniques for interpolation in graph structured data,” in *Acoustics, Speech and Signal Processing (ICASSP), 2013 IEEE International Conference on*, May 2013, pp. 5445–5449.
- [8] S. Chen, R. Varma, A. Sandryhaila, and J. Kovacevic, “Discrete signal processing on graphs: Sampling theory,” *CoRR*, vol. abs/1503.05432, 2015. [Online]. Available: <http://arxiv.org/abs/1503.05432>
- [9] X. Wang, P. Liu, and Y. Gu, “Local-set-based graph signal reconstruction,” *Signal Processing, IEEE Transactions on*, vol. 63, no. 9, pp. 2432–2444, May 2015.
- [10] D. Shuman, B. Ricaud, and P. Vandergheynst, “A windowed graph fourier transform,” in *Statistical Signal Processing Workshop (SSP), 2012 IEEE*, Aug 2012, pp. 133–136.
- [11] N. Tremblay, P. Borgnat, and P. Flandrin, “Graph empirical mode decomposition,” in *Signal Processing Conference (EUSIPCO), 2014 Proceedings of the 22nd European*, Sept 2014, pp. 2350–2354.
- [12] D. Shuman, C. Wiesmeyr, N. Holighaus, and P. Vandergheynst, “Spectrum-adapted tight graph wavelet and vertex-frequency frames,” *Signal Processing, IEEE Transactions on*, vol. PP, no. 99, pp. 1–1, 2015.
- [13] N. Leonardi and D. Van De Ville, “Tight wavelet frames on multislice graphs,” *Signal Processing, IEEE Transactions on*, vol. 61, no. 13, pp. 3357–3367, July 2013.
- [14] R. Coifman and M. Maggioni, “Diffusion wavelets,” *Applied and Computational Harmonic Analysis*, vol. 21, no. 1, pp. 53–94, 2006.
- [15] S. Narang and A. Ortega, “Perfect reconstruction two-channel wavelet filter banks for graph structured data,” *Signal Processing, IEEE Transactions on*, vol. 60, no. 6, pp. 2786–2799, June 2012.
- [16] A. Sakiyama and Y. Tanaka, “Oversampled graph Laplacian matrix for graph filter banks,” *Signal Processing, IEEE Transactions on*, vol. 62, no. 24, pp. 6425–6437, Dec 2014.
- [17] H. Nguyen and M. Do, “Downsampling of signals on graphs via maximum spanning trees,” *Signal Processing, IEEE Transactions on*, vol. 63, no. 1, pp. 182–191, Jan 2015.
- [18] V. Ekambaram, G. Fanti, B. Ayazifar, and K. Ramchandran, “Critically-sampled perfect-reconstruction spline-wavelet filterbanks for graph signals,” in *Global Conference on Signal and Information Processing (GlobalSIP), 2013 IEEE*, Dec 2013, pp. 475–478.
- [19] H. Behjat, N. Leonardi, L. Sornmo, and D. Van De Ville, “Canonical cerebellar graph wavelets and their application to fmri activation mapping,” in *Engineering in Medicine and Biology Society (EMBC), 2014 36th Annual International Conference of the IEEE*, Aug 2014, pp. 1039–1042.
- [20] N. Tremblay and P. Borgnat, “Graph wavelets for multiscale community mining,” *Signal Processing, IEEE Transactions on*, vol. 62, no. 20, pp. 5227–5239, Oct 2014.
- [21] S. Narang, Y. H. Chao, and A. Ortega, “Graph-wavelet filterbanks for edge-aware image processing,” in *Statistical Signal Processing Workshop (SSP), 2012 IEEE*, Aug 2012, pp. 141–144.
- [22] G. Strang and T. Nguyen, *Wavelets and filter banks*. SIAM, 1996.
- [23] S. Fortunato, “Community detection in graphs,” *Physics Reports*, vol. 486, no. 3–5, pp. 75–174, 2010.
- [24] F. Chung, *Spectral graph theory*. Amer Mathematical Society, 1997, no. 92.
- [25] S. Narang and A. Ortega, “Compact support biorthogonal wavelet filterbanks for arbitrary undirected graphs,” *Signal Processing, IEEE Transactions on*, vol. 61, no. 19, pp. 4673–4685, Oct 2013.
- [26] D. I. Shuman, M. J. Faraji, and P. Vandergheynst, “A framework for multiscale transforms on graphs,” *CoRR*, vol. abs/1308.4942, 2013. [Online]. Available: <http://arxiv.org/abs/1308.4942>
- [27] B. Aspvall and J. R. Gilbert, “Graph coloring using eigenvalue decomposition,” *SIAM Journal on Algebraic Discrete Methods*, vol. 5, no. 4, pp. 526–538, 1984. [Online]. Available: <http://dx.doi.org/10.1137/0605051>
- [28] F. Dorfler and F. Bullo, “Kron reduction of graphs with applications to electrical networks,” *Circuits and Systems I: Regular Papers, IEEE Transactions on*, vol. 60, no. 1, pp. 150–163, Jan 2013.
- [29] G. Karypis and V. Kumar, “A fast and high quality multilevel scheme for partitioning irregular graphs,” *SIAM Journal on Scientific Computing*, vol. 20, no. 1, pp. 359–392, 1998. [Online]. Available: <http://dx.doi.org/10.1137/S1064827595287997>
- [30] S.-H. Teng, “Coarsening, sampling, and smoothing: Elements of the multilevel method,” in *Algorithms for Parallel Processing*, ser. The IMA Volumes in Mathematics and its Applications. Springer New York, 1999, vol. 105, pp. 247–276.
- [31] R. Band, I. Oren, and U. Smilansky, “Nodal domains on graphs - how to count them and why?” *Analysis on Graphs and its applications Proc. Symp. Pure Math.*, 2008.

- [32] V. Blondel, J. Guillaume, R. Lambiotte, and E. Lefebvre, "Fast unfolding of communities in large networks," *Journal of Statistical Mechanics: Theory and Experiment*, vol. 2008, no. 10, p. P10008, 2008.